Two-phase dynamical equilibria driven by irradiation in ordered alloys

F. Soisson, P. Bellon, and G. Martin
Section de Recherches de Métallurgie Physique, CEREM, Centre d'Etudes de Saclay, F-91191 Gif-sur-Yvette CEDEX, France
(Received 16 March 1992)

We study here two-phase equilibria in driven compounds, where two dynamics are acting in parallel: thermally activated atomic jumps and forced jumps; such is the case for an alloy under irradiation where nuclear collisions induce ballistic jumps. We propose a deterministic treatment of the concentration and degree of order fields (one or two dimensional) and identify two-phase locally stable steady states: Dynamical equilibrium phase diagrams are thus computed. It is shown that in a body-centered-cubic alloy an $A2$-$B2$ order-disorder transition of the second kind at thermal equilibrium becomes of the first kind beyond a temperature-dependent critical forcing intensity. As a result, two-phase steady states can be stabilized by irradiation. Interface properties are then studied: Surface-tension-like effects are observed; introduction of antiphase boundaries destabilizes ordered precipitates, leading to their dissolution and redistribution. In order to compare the relative stability of the different steady states, a stochastic description is then proposed: We build a mean-field grand-canonical potential which governs the steady-state probability distribution of the concentration and long-range order parameter. It shows that the most stable steady state is indeed two-phase under suitable irradiation conditions.

I. INTRODUCTION

As is well known, irradiation by energetic particles can enhance or induce phase transitions: Amorphization of crystalline solids, disordering of ordered alloys, dissolution of precipitates, or irradiation-induced precipitation in a solid solution are good examples (for a review, see Ref. 1). These can be reviewed as dynamical phase transitions in driven systems:[2-6] Indeed, in a solid under irradiation, nonequilibrium configurations are sustained by the permanent injection of Frenkel pairs and of replacement collisions (ballistic jumps). Such irradiation-induced phase transitions have an important technological impact: Extrapolating data obtained for one set of irradiation conditions to yet-unexplored irradiating environments (e.g., 14-MeV neutron irradiation) cannot be done straightforwardly and requires modeling.

Here we focus on ordered alloys: In most simple cases, the state of the system results from competition between the disordering due to the ballistic jumps induced by nuclear collisions and the reordering due to the thermally activated jumps of point defects.[7,8] Kinetic models, based on rate theory and incorporating these competing two effects, have long been used for fitting disordering or ordering rates measured experimentally.[9,10] However, as soon as two or more locally stable steady states are competing, such descriptions do not provide any information on their relative stability. Furthermore, some relevant effects such as the production of ballistic jumps by bursts cannot be addressed by these models (cascade-size effect).

A kinetic description we introduced recently allows one to address such questions: Starting from a master equation, stochastic potentials can be computed; they play a role analogous to thermodynamic potentials for equilibrium systems and permit one to construct *dynamical equilibrium* phase diagrams in a (temperature $\times$concentration$\times$irradiation flux) space. Up to now, this technique has been applied to a homogeneous description of ordering-disordering on face-centered-cubic (fcc) or body-centered-cubic (bcc) lattices: It has been successful in rationalizing subtle inversion of stability and bistability effects observed in Ni_4Mo during 1-MeV electron irradiation;[11] it has predicted that various nonequilibrium phases can be stabilized by irradiation depending on the saddle-point configuration energy in atomic diffusion[12] and the shift in the $A2$-$B2$ transition from second to first order beyond a threshold in irradiation flux, with a sensitivity of first-order transition lines to replacement cascade size.[13] Thus, in the latter case, phase coexistence is expected to be induced by irradiation for nonstoichiometric compositions.

In this paper we address the problem of phase coexistence under irradiation for coherent ordered precipitates: We consider a binary A_cB_{1-c} alloy on a bcc lattice under irradiation, where two phases at different compositions can coexist in dynamical equilibrium. In Sec. II homogeneous and heterogeneous deterministic kinetic descriptions are used for building steady-state stability diagrams and for studying interfacial properties. In Sec. III, after a brief recall of the stochastic description introduced elsewhere,[11,13] a grand-canonical ensemble is proposed, from which a global-stability criterion is obtained: A dynamical equilibrium phase diagram can then be built. The work presented here is done in the simplest mean-field approximation ("point approximation"), which has already yielded useful and unexpected results. More sophisticated treatments are possible (pair or higher approximation, Monte Carlo simulations[14]) and are left for future work.

II. DETERMINISTIC KINETIC DESCRIPTION

We study here the $A2$-$B2$ transition driven on a bcc lattice. A homogeneous model is first used to show that the transition becomes first order beyond a critical driv-

ing, while it is second order at equilibrium. Then a heterogeneous description allows the study of interfacial properties of the two-phase state induced by external forcing.

A. Homogeneous model

We consider a binary A_cB_{1-c} alloy on a rigid bcc lattice and focus on the $B2$-$A2$ order-disorder transition: A Bragg-Williams approximation is then appropriate.[15] For $B2$ ordering, it is convenient to decompose the bcc lattice into two simple cubic sublattices α and β. The state of order is then described by the atomic concentrations C^α and C^β on both sublattices or by the average concentration C and the degree of long-range order $S=2(C^\alpha-C)=-2(C-C^\beta)$. We restrict discussion to nearest-neighbor interactions, so that the order-disorder transition is of second order at equilibrium.[14] The ordering energy is $\omega=(z/2)(V_{aa}+V_{bb}-2V_{ab})$, where V_{ij} is the energy of a pair of i-j atoms (for ordering systems $\omega>0$) and z is the coordination number ($z=8$).

1. *Diffusion model*

We model atomic diffusion by permuting two nearest-neighbor atoms belonging to distinct sublattices according to two mechanisms operating in parallel: (i) ballistic jumps induced by nuclear collisions at a frequency Γ_b, which is independent of the state of order of the system and its temperature, and (ii) thermally activated jumps. According to rate theory, the activation energy $E^{\rm act}_{\alpha\beta}$ ($E^{\rm act}_{\beta\alpha}$) is the energy necessary to extract an $A_\alpha B_\beta$ pair ($A_\beta B_\alpha$) from its environment, where its energy is $E_{\alpha\beta}$ ($E_{\beta\alpha}$) and to bring it into a saddle-point position where its energy is E_s (Fig. 1). E_s is assumed to be independent of the surrounding of the AB pair.

The exchange of an A atom on the sublattice α with a B atom on the sublattice β occurs at the frequency

$$\Gamma_{\alpha\beta}=\Gamma^{\rm th}_{\alpha\beta}+\Gamma_b=\nu\exp\left[-\frac{E^{\rm act}_{\alpha\beta}}{kT}\right]+\Gamma_b \tag{1}$$

and the inverse exchange at the frequency

$$\Gamma_{\beta\alpha}=\Gamma^{\rm th}_{\beta\alpha}+\Gamma_b=\nu\exp\left[-\frac{E^{\rm act}_{\beta\alpha}}{kT}\right]+\Gamma_b\ . \tag{2}$$

Note that, in this model, the system "knows" which state it is leaving but "ignores" the state it is moving to, beyond the saddle point. It is sometimes assumed[16,17] that the activation energy is a fraction of the energy difference between final and initial states: This would only affect the kinetics of a thermal system ($\Gamma_b=0$), but would modify the steady states of a driven one ($\Gamma_b\neq0$). Our choice is more appropriate to far-from-equilibrium systems.

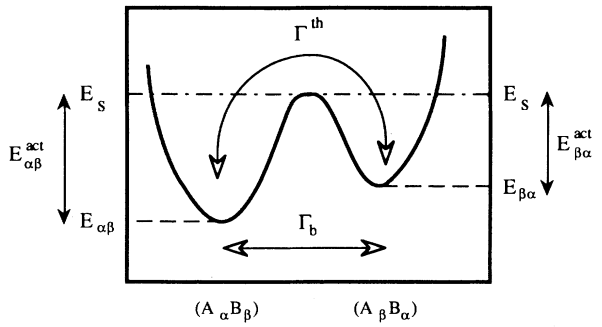

FIG. 1. Schematic variation of internal energy during atomic exchange with two mechanisms operating in parallel: ballistic and thermally activated jumps. See Eqs. (1) and (2) for the definition of the jump frequencies Γ_b and $\Gamma^{\rm th}$.

In the Bragg-Williams approximation, the energy for the extraction of an AB pair in a broken bound model is

$$E_{\alpha\beta}=E_s-8(V_{ab}+V_{bb})-8(V_{aa}-V_{bb})C-\omega S\ , \tag{3}$$

$$E_{\beta\alpha}=E_s-8(V_{ab}+V_{bb})-8(V_{aa}-V_{bb})C+\omega S\ , \tag{4}$$

leading to

$$\Gamma_{\alpha\beta}=\Gamma_t\exp(-2ST_c/T)+\Gamma_b\ , \tag{5}$$

$$\Gamma_{\beta\alpha}=\Gamma_t\exp(+2ST_c/T)+\Gamma_b\ , \tag{6}$$

with $T_c=\omega/2k$ and where Γ_t is an averaged frequency for thermal jumps.

The time evolution of the system is given by

$$\frac{dC^\alpha}{dt}=-8\Gamma_{\alpha\beta}C^\alpha(1-C^\beta)+8\Gamma_{\beta\alpha}C^\beta(1-C^\alpha) \tag{7}$$

or by

$$\frac{dS}{dt}=f(S)=-16\Gamma_{\alpha\beta}\left\{C(1-C)+\frac{S}{2}+\frac{S^2}{4}\right\}+16\Gamma_{\beta\alpha}\left\{C(1-C)-\frac{S}{2}+\frac{S^2}{4}\right\}\ . \tag{8}$$

For the sake of simplicity, we set $V_{aa}=V_{bb}$ for all numerical applications in Sec. II. By symmetry arguments, we can restrict ourselves to the case $0\le C\le0.5$.

2. *Thermal system* ($\Gamma_b=0$)

As required, the kinetic equation (7) or (8) drives a thermal system toward its equilibrium state as predicted from thermodynamics. Indeed, the steady-state concentration is solution of $dC^\alpha/dt=0$: This equation is identical to that obtained by extremizing the Bragg-Williams free energy per site:[13]

$$\mathcal{F}(C^\alpha,C^\beta)=-\omega C(1-C)-\frac{\omega}{4}(C^\alpha-C^\beta)^2+4V_{bb}+4(V_{aa}-V_{bb})C+\frac{kT}{2}\{C^\alpha\ln C^\alpha+(1-C^\alpha)\ln(1-C^\alpha)+C^\beta\ln C^\beta+(1-C^\beta)\ln(1-C^\beta)\}\ . \tag{9}$$

The order-disorder transition is of the second kind with a critical temperature T_c for an average composition $C=0.5$.

3. *Driven system* ($\Gamma_b \neq 0$)

We define a Lyapunov function $\mathcal{L}$ by $\partial\mathcal{L}/\partial S=-f(S)$ and study it in the spirit of Landau's theory of phase transitions.[18] The function f has vanishing odd derivatives at the disordered state ($S=0$), and the critical temperature at the composition C is defined by $(\partial f/\partial S)_{S=0}=0$. The transition is of the second kind for $(\partial^3 f/\partial S^3)_{S=0}<0$ and of the first kind for $(\partial^3 f/\partial S^3)_{S=0}>0$.

Then the homogeneous disordered solution ($S=0$) is stable above

$$\frac{T^*}{T_c}=4\frac{C(1-C)}{1+\gamma} , \tag{10}$$

with

$$\gamma=\frac{\Gamma_b}{\Gamma_t} . \tag{11}$$

The transition becomes first order for $(\partial^3 f/\partial S^3)_{S=0}=0$, i.e.,

$$\frac{T^*}{T_c}=\frac{8C(1-C)}{3+\sqrt{9-24C(1-C)}} \tag{12a}$$

and

$$\gamma^*=\frac{\sqrt{9-24C(1-C)}+1}{2} . \tag{12b}$$

Beyond this tricritical line, a two-phase alloy is expected (coexistence between the ordered and disordered phase). These results are summarized in a steady-state diagram in the $T/T_c, C, \gamma$ space, as shown in Fig. 2.

B. Heterogeneous model

In order to follow the spatial behavior of the two-phase system, we first define a *local concentration* on each sublattice. In order to derive the mean-field approximation consistently, we consider one- or two-dimensional problems where the concentrations on each sublattice are defined by averaging the occupancy on lattice planes or atomic rows perpendicular to the diffusion direction or plane, respectively.

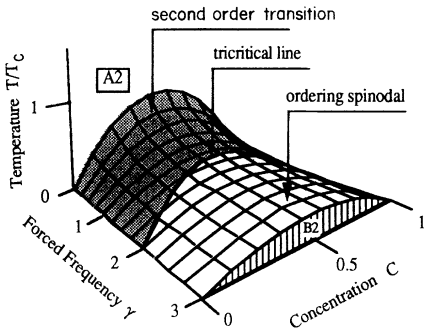

FIG. 2. Dynamical equilibrium phase diagram for a bcc alloy in ($T\times\gamma\times C$) space. For clarity, when the transition is first order, only the spinodal is displayed. γ is dimensionless Eq. (11).

Extending the kinetic model described in the previous section, the jump frequencies are now

$$\Gamma^{ij}_{\alpha\beta}=\nu\exp\left[-\frac{E^{ij}_{\alpha\beta}}{kT}\right]+\Gamma_b , \tag{13}$$

$$\Gamma^{ji}_{\beta\alpha}=\nu\exp\left[-\frac{E^{ji}_{\beta\alpha}}{kT}\right]+\Gamma_b , \tag{14}$$

with

$$E^{ij}_{\alpha\beta}=E_s-\sum_{p}^{nn(i)}\{C_p^{\beta}V_{aa}+(1-C_p^{\beta})V_{ab}\} - \sum_{q}^{nn(j)}\{C_q^{\alpha}V_{ab}+(1-C_q^{\alpha})V_{bb}\} \tag{15}$$

(and the analogous expression for $E^{ji}_{\beta\alpha}$).

C_q^{α} and C_p^{β} are, respectively, the A atomic concentrations on the sublattices α and β at the locations q and p; i and j run from 1 to the number of cells n_c. The summations in Eq. (15) are restricted to nearest neighbors of sites i and j [$nn(i)$ and $nn(j)$, respectively].

The rate of change of concentration on the sublattice α at location i is

$$\frac{dC_i^{\alpha}}{dt}=\sum_{j}^{nn(i)}\{-\Gamma^{ij}_{\alpha\beta}C_i^{\alpha}(1-C_j^{\beta})+\Gamma^{ji}_{\beta\alpha}C_j^{\beta}(1-C_i^{\alpha})\} . \tag{16}$$

A similar expression holds for dC_j^{β}/dt with α and β interchanged.

As for the homogeneous model, the control parameters are the reduced temperature T/T_c, the average concentration C, and the reduced forced frequency γ. The evolution of the system as well as its steady states are obtained by numerical integration of Eq. (16) using periodic boundary conditions, for different sets of initial conditions $\{C_i^{\alpha}(t=0),\ C_i^{\beta}(t=0)\}$.

Typical numbers of bcc cells are $n_c=40$–400 for one-dimensional computations and $n_c=40\times40$ to 80×80 for two-dimensional ones. The fourth-order Runge-Kutta method with adaptive step-size control[19] was found to be the most efficient. The relative error of the concentrations is kept less than 10^{-6} during each integration step, and the stationary state is assumed to be reached when all the time derivatives are less than 10^{-8}.

1. *Steady-state stability diagrams*

Beyond the tricritical line, various locally stable steady states may exist for the same values of T/T_c, C, and γ: They are identified by varying the initial conditions.

With homogeneous initial conditions, three domains can be defined: For large values of T/T_c or γ, only the homogeneous disordered solution $\{C_i^{\alpha}=C_i^{\beta}=C\}$ is stable, while for low values only the homogeneous ordered solution is stable, and for intermediate values these two solutions are both locally stable (Fig. 3).

With heterogeneous initial conditions, a two-phase al-

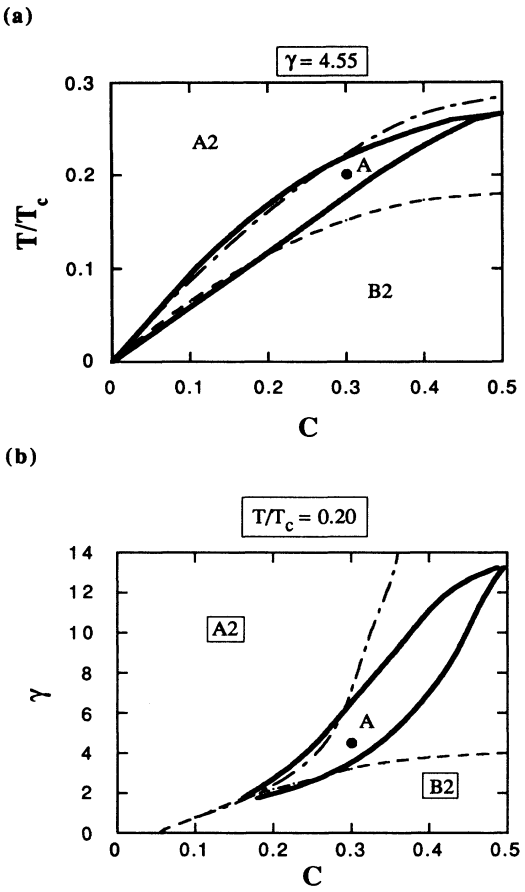

FIG. 3. (a) Isoforcing and (b) isothermal cuts of the steady-state stability diagram: ordering spinodal line (dashed line), disordering spinodal line (dot-dashed line), and limits of the two-phase field (solid line). γ is dimensionless.

loy can be stabilized: An ordered phase coexists with a solute-depleted disordered one. The respective proportion of the two phases fulfills the lever rule: Changing the average concentration changes the proportion of both phases without affecting their own composition. Two examples of steady-state diagrams so obtained are displayed in Figs. 3(a) and 3(b) (one for a given forcing and one for a given temperature). As will be seen later, the assessment of the relative stability of various steady states requires a stochastic description (where fluctuations are taken into account), but their local stability in response to a given perturbation can be studied.[20] For instance, consider a system which at steady state can be either homogeneously ordered or two phased [its representative point—as point A in Fig. 3—lies in the two-phase field and below the ordering spinodal in the steady-state $(T/T_c, C, \gamma)$ diagram]. The introduction of an antiphase boundary (APB) in an initially ordered homogeneous steady state induces a decomposition into two phases: The latter steady state could therefore be the most stable.

The parameter $\gamma=\Gamma_b/\Gamma_t$ is a function of Γ_b and T/T_c (and of the composition C if $V_{aa}\neq V_{bb}$). Γ_t is proportional to the mean point-defect concentration, which depends on the irradiation flux and temperature. Assuming that a steady-state point-defect concentration is obtained by Frenkel-pair mutual recombination, γ is given by[13]

$$\gamma=g\left[\frac{\Gamma_b}{\Gamma_v}\right]^{1/2}. \tag{17}$$

Here g is a geometrical factor and Γ_v is the mean vacancy jump frequency:

$$\Gamma_v=\Gamma_v^0\exp\left[-\frac{E_v^m}{kT}\right], \tag{18}$$

where E_v^m is the vacancy migration energy. Then, with $\gamma_0=g(\Gamma_b/\Gamma_v^0)^{1/2}$, we get

$$\gamma=\gamma_0\exp\left[\frac{E_v^m}{2kT}\right]. \tag{19}$$

When a quasi-steady-state regime is assumed for point defects,[21] it is easily shown that a similar expression holds, but with the interstitial migration energy E_i^m entering in Eq. (19) instead of E_v^m.

The irradiation conditions can be defined by T/T_c, C, and γ_0, and an isoforcing steady-state diagram can be drawn at γ_0 constant (instead of γ constant) as in experimental conditions where irradiation flux (which scales Γ_b) and temperature are adjusted independently. Such a diagram is displayed in Fig. 4, with $\gamma_0=10^{-5}$ and a typical value $E_d^m=0.5$ eV for defect migration energy.

2. *Surface-tension effects*

The heterogeneous model is suitable for studying interfacial properties of the two-phase system and its spatial behavior.

A surface-tension-like effect is identified: The A atomic concentration in both phases depends on the precipitate radius R (Fig. 5); as for a thermal system, the relative increase of composition in the precipitate and matrix with respect to the compositions for a planar interface is proportional to R^{-1} for small R^{-1} values.

Consistently with this effect, the system is found to exhibit coarsening. We start the computation with two ordered precipitates with a different curvature in the computation cell. Each of them is initially surrounded by a

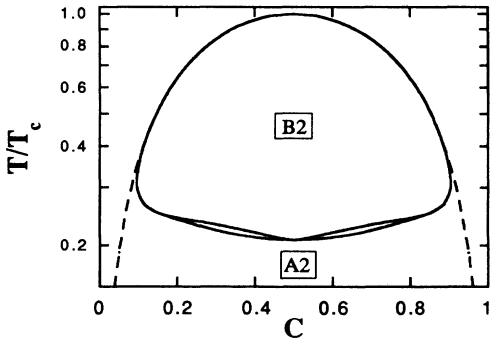

FIG. 4. Steady-state stability diagram with γ_0 constant. Defect migration energy $E_d^m=0.5$ eV. $\gamma_0=10^{-5}$ (solid line) and $\gamma_0=0$ (equilibrium phase diagram) (dashed line).

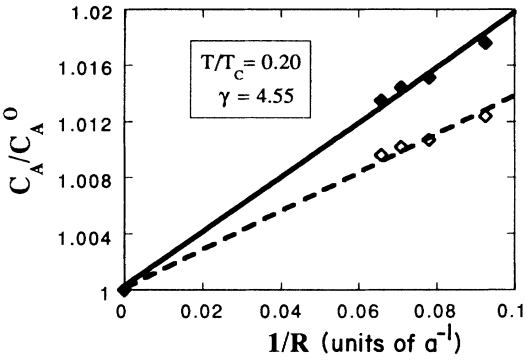

FIG. 5. *A* atomic concentrations in the ordered (solid line) and disordered (dashed line) phases which coexist in dynamical equilibrium as a function of the radius of curvature of the ordered precipitate: The concentrations are scaled to their respective values for a planar interface.

disordered phase, the composition of which is the steady-state value obtained with a single precipitate alone. A diffusion flux is then induced which equalizes the composition in the whole disordered phase, and the larger precipitate coarsens, while the smaller one shrinks and disappears: We conclude that, at this scale ($n_c \leq 80 \times 80$), no patterning is expected in the model.

Moreover, in the two-dimensional description, as far as we could check, "spherical" precipitates are always observed, with no faceting, contrary to a thermal two-phase system. A systematic study is beyond the scope of this paper and is left for future work.

3. *Redistribution of antiphased precipitates*

The deterministic evolution equations (16) allow one to follow the kinetic path of systems prepared in nonsteady-state configurations. As a matter of illustration, we studied the reaction of an ordered precipitate to the presence of an antiphase boundary, as it would be the case after shearing by a dislocation.

Figure 6 shows a two-phase alloy stabilized by irradiation ($T/T_c = 0.20$, $\gamma = 4.55$) and its evolution after introduction of an APB in the ordered precipitate, along a $\langle 110 \rangle$ direction. A disordered region is found to grow at the APB: The solid solution invades the APB, and the two antiphased precipitates repel each other by a dissolution-redeposition mechanism. Finally, the smaller ordered precipitate shrinks and disappears to the benefit of the larger one. The evolution is qualitatively the same with a conservative $\{110\}$ or a nonconservative $\{100\}$ APB. Note that the ordered precipitate center moved during the process.

In order to compare this behavior with that of a thermal two-phase system, second-neighbor interactions must be taken into account in the Bragg-Williams approximation. We call $V^{(1)}$ and $V^{(2)}$ the ordering energy for interactions between nearest and next-nearest neighbors, respectively. For particular values of the composition, temperature, and parameter $V = V^{(1)}/V^{(2)}$, a two-phase alloy can be stable without forcing[22] (here we set $V = \frac{4}{3}$). Equations (10)–(13) can then be generalized to take into account second-neighbor interactions, and the same numerical techniques are used to compute the steady state. After its introduction in such a two-phase alloy ($T/T_c = 0.25$ and $\gamma = 0$), the APB tends to align along a $\langle 100 \rangle$ direction (Fig. 7) by a process where the migration of interface steps plays a crucial role. If the APB is initially introduced along a $\langle 100 \rangle$ direction, no significant evolution is observed (Fig. 8), the system remaining trapped into a metastable state. If we now increase the temperature ($T/T_c = 0.5$), we note a rounding of the ordered precipitate and the evolution of the thermal system after the APB introduction becomes similar to the one displayed in Fig. 6 for a driven system. Therefore the isotropy of the surface tension is thought to be at the origin of the APB elimination mechanism.

Under irradiation, the high-temperature boundary of the two-phase field is lowered as γ increases (similarly to what is observed in Fig. 2). As a result, keeping constant the temperature and composition and increasing γ, the representative point of the irradiation parameters becomes close to this boundary. In a purely thermal system, such a shift can be done by increasing the temperature. We observed that the elimination of the APB indeed proceeds in a similar way in the two cases: ($T/T_c = 0.25$, $\gamma = 0$) and ($T/T_c = 0.20$, $\gamma = 4.55$). The introduction of ballistic jumps can be viewed as increasing the temperature of the system. This is reminiscent of the effective temperature criterion introduced by Martin for unmixing under irradiation.[7]

Despite its interest, the deterministic description used up to now suffers strong drawbacks. In particular, the system will remain trapped in any locally stable state: This is the case for the equilibrium two-phase alloy with an APB in Fig. 8. In a real system, the existence of fluctuations will finally allow the APB elimination, so that the system can reach its absolute minimum in free energy.

III. STOCHASTIC DESCRIPTION

The deterministic kinetic description introduced in the above paragraph allows one to compute the possible locally stable steady states of the system under irradiation. However, this description does not give any information on the relative stability of competing steady states when several exist: Indeed, the lifetime of metastable states is governed by the fluctuations which are absent from this deterministic treatment. We will now introduce a stochastic kinetic description,, which includes the fluctuations, and show that from this stochastic description one can compute stochastic potentials which generalize thermodynamic potentials. Using such stochastic potentials, one assesses the relative stability of competing steady states and builds dynamical equilibrium phase diagrams. In Sec. III A we recall this stochastic description for canonical homogeneous systems, and in Sec. III B we show how to build a grand-canonical homogeneous description, so as to address the coexistence between phases at different compositions as observed in Sec. II B.

A. Homogeneous canonical stochastic description

1. Master equation

This description has been introduced in Refs. 11, 13, and 23. We recall briefly the procedure here. Considering a homogeneous crystal at a fixed composition C consisting of Ω sites on each sublattice α and β, we define the state of the system by the number of A atoms on α sublattice N^{α}. Let $P(N^{\alpha},t)$ be the probability of the value N^{α} at time t for given initial conditions. For the Marko-

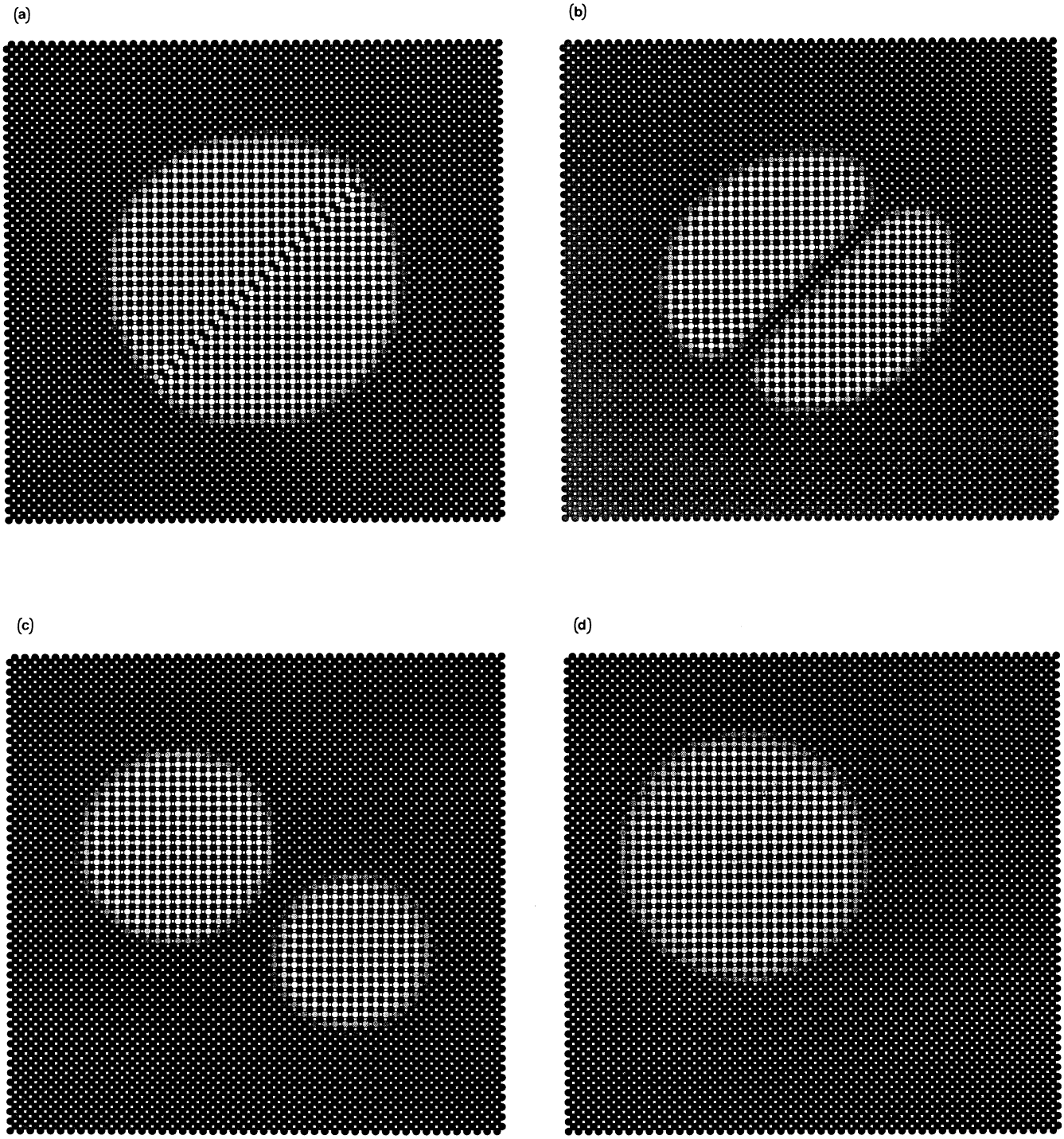

FIG. 6. Evolution of an ordered precipitate after a conservative APB introduction in a thermal system. $T/T_c=0.25$ and $\gamma=0$. The concentrations at lattice sites are visualized by the darkness of the circles. The maxima of A atomic concentrations (here close to 0.98) are represented by the darkest circles, and the minima (here close to 0.02) are represented by the lightest circles. In arbitrary time units (a) $t=0$, (b) $t=1$, (c) $t=300$, and (d) $t=900$.

vian processes considered here, the time evolution of $P(N^\alpha,t)$ is governed by the master equation[24,25]

$$\frac{dP}{dt}(N^\alpha,t)=\sum_{k=1}^{b}\{-P(N^\alpha,t)[W(N^\alpha,-k)+W(N^\alpha,+k)] +P(N^\alpha-k,t)W(N^\alpha-k,+k) +P(N^\alpha+k,t)W(N^\alpha+k,-k)\} . \quad (20)$$

$W(N^\alpha,+k)$ is the transition rate at which systems having N^α A atoms on sublattice α reach the state $N^\alpha+k$ because of atomic exchanges: For thermally activated jumps, the only possible values for k are ± 1, while for the ballistic jumps induced by nuclear collisions, b (and therefore k) can be larger than 1 (effect of replacement cascades). In the following we restrict ourselves to the simple case where ballistic jumps are assumed to occur individually (cascade-size effects have been treated for the

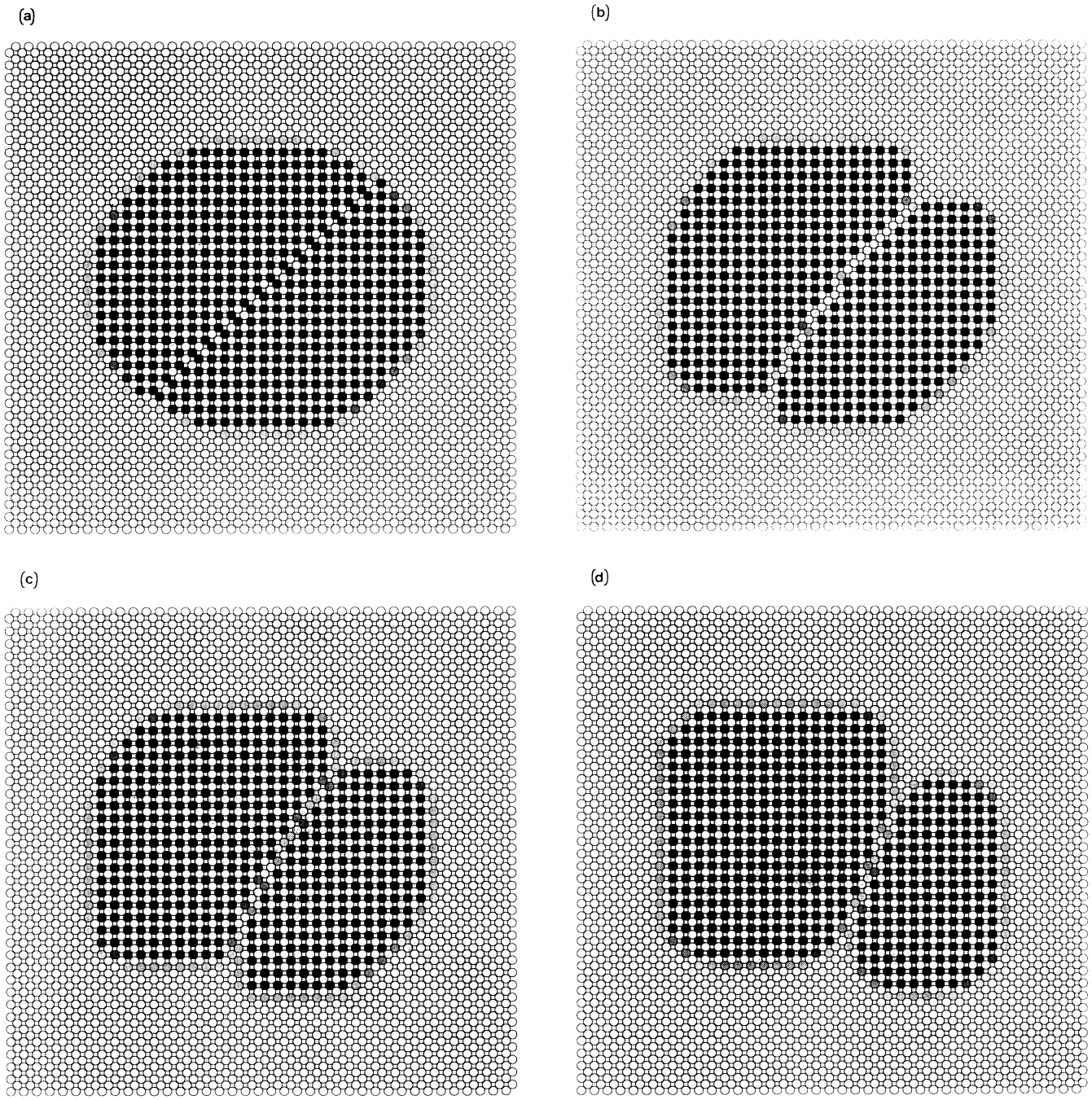

FIG. 7. Evolution of an ordered precipitate after conservative APB introduction in a driven system. $T/T_c=0.20$ and $\gamma=4.55$. The concentrations at lattice sites are visualized by the darkness of the circles. The maxima of A atomic concentration (here close to 0.67) are represented by the darkest circles, and the minima (here close to 0.01) are represented by the lightest circles. In arbitrary time units (a) $t=0$, (b) $t=1760$, (c) $t=2660$, and (d) $t=8960$.

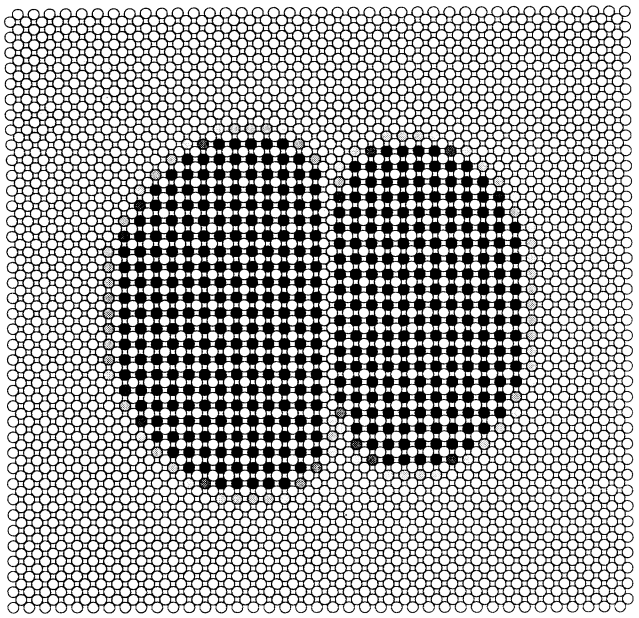

FIG. 8. Steady-state ordered precipitate after a nonconservative APB introduction in a thermal system. $T/T_c=0.25$ and $\gamma=0$.

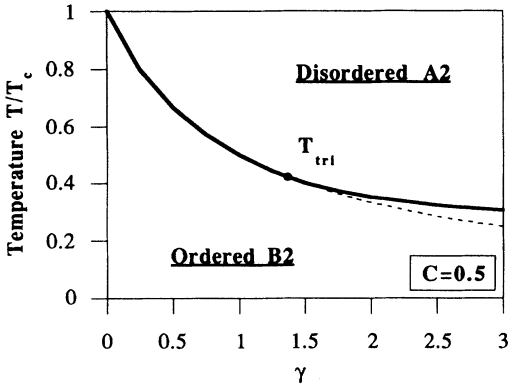

FIG. 9. Dynamical equilibrium phase diagram for $C=0.5$, as computed from the potential Φ solution of the master equation. γ is dimensionless.

equiatomic composition in Refs. 13 and 26). The transition rates entering Eq. (20) are the sum of the thermal and ballistic contributions, which can be constructed from the atomistic jump frequencies $\Gamma^{\rm th}_{\alpha\beta}$ and $\Gamma^{\rm th}_{\beta\alpha}$ and the ballistic jump frequency Γ_b introduced in Sec. II:

$$W(N^\alpha,\pm k)=W^{\rm th}(N^\alpha,\pm k)+W^b(N^\alpha,\pm k)\ , \tag{21}$$

$$\begin{aligned} &W^{\rm th}(N^\alpha,+1)=8\Omega C^\beta(1-C^\alpha)\Gamma^{\rm th}_{\beta\alpha}\ , \\ &W^b(N^\alpha,+1)=8\Omega C^\beta(1-C^\alpha)\Gamma_b\ , \end{aligned} \tag{22a}$$

$$\begin{aligned} &W^{\rm th}(N^\alpha,-1)=8\Omega C^\alpha(1-C^\beta)\Gamma^{\rm th}_{\alpha\beta}\ , \\ &W^b(N^\alpha,-1)=8\Omega C^\alpha(1-C^\beta)\Gamma_b\ . \end{aligned} \tag{22b}$$

In Eqs. (22), $\Gamma^{\rm th}_{ij}$ is a function of $C^\alpha=N^\alpha/\Omega$ (or of S), as defined by Eqs. (1) and (2). We are interested in the steady-state solution of Eq. (20). The latter is a conservation equation for the probability at each "site" of the N^α axis, so that the right-hand side (RHS) of Eq. (20) may be considered as the difference between the net flux of probability between sites $N^\alpha-1$ and N^α, on the one hand, and N^α and $N^\alpha+1$, on the other hand. Since systems with $N^\alpha=0$ or Ω can be neither created nor destroyed, each of the above fluxes must be zero under steady-state conditions. We get

$$P(N^\alpha)W(N^\alpha,+1)=P(N^\alpha+1)W(N^\alpha+1,-1)\ . \tag{23}$$

Note that the latter equation is particularly simple: It is the detailed balance property for the mesoscopic variable N^α. This is very specific to the simple case treated here where the state of the system is described by the scalar order parameter N^α and where only single-step processes ($b=1$) are considered.

Under irradiation, both thermal jumps and single ballistic jumps are operating: Iterating Eq. (23) between $N^\alpha=N$ and $\Omega/2$, simple algebra leads to

$$\frac{P(N)}{P(\Omega/2)}=\exp\{2\Omega[\psi(S)-\psi(\tfrac{1}{2})]\}\ , \tag{24}$$

where the stochastic potential ψ only depends on the intensive variable (C or S). ψ is the sum of two terms: a configurational entropy term and another term which combines energetics (T_c/T) and kinetics (Γ_b/Γ_t). This latter term is by no means an internal energy term.[11,12]

We have checked analytically that in the absence of irradiation $\psi=-\mathcal{F}/kT$ [$\mathcal{F}$ is the free energy defined by Eq. (9)]: This kinetic model yields the same probability distribution as the thermodynamic one.[13]

From the knowledge of $\psi(S)$, the respective stability of possible steady states can be assessed: The most stable steady-state configuration corresponds to the absolute maximum of ψ. In the stoichiometric case ($c=0.5$), only homogeneous steady states are competing and the stability boundary between the ordered and disordered states is computed,[13] as displayed in Fig. 9. As derived by Görtz under some general conditions,[27] the extrema of ψ are found to coincide with the steady states of the deterministic equation (7), which corresponds to the first moment of the master equation (20). The high- and low-temperature limits of the bistability domain in Fig. 3(a) at $c=0.5$ correspond to spinodal temperatures of the ordered and disordered states, respectively, of the potential ψ.

2. *Kubo-Matsuo-Kitihara ansatz*

When the order parameter is not a scalar[12] or when replacement cascades are operating ($b\neq1$),[11] the equation obtained under steady-state conditions for the master equation becomes much more complex than Eq. (23), and an analytical solution is no longer available. Kubo, Matsuo, and Kitihara[28] and Suzuki[29] have shown how to approximate the master equation in the large system-size limit: We assume that $P(\mathcal{N},t)$ exhibits the extensive property $P(\mathcal{N},t)\propto\exp\{2\Omega\Phi(\mathcal{N},t)\}$, where $\nu=\mathcal{N}/\Omega$.[30] In Eq. (20), assuming that Φ is continuously differentiable and expanding all functions evaluated at $\nu\cdot\varepsilon/\Omega$ around their value at ν to first order in Ω^{-1}, one gets the Kubo-

Matsuo-Kitihara equation for the potential Φ:

$$\frac{\partial\Phi(\mathcal{N},t)}{\partial t}=\sum_{\varepsilon} w(\mathcal{N},\varepsilon)\{\exp[-(\varepsilon\cdot\nabla)2\Phi]-1\}\ , \quad (25)$$

where $w(\mathcal{N},\varepsilon)$ is the transition rate defined by $w(\mathcal{N},\varepsilon)=w(\mathcal{N},\varepsilon)2\Omega$ and $\Phi(\mathcal{N})$ will denote the solution of Eq. (25) under steady-state conditions. It is easily checked that, for the simple example described above, the analytical expressions for the potentials Φ and Ψ are identical. In complex cases (Refs. 12 and 26 and below), the Kubo-Matsuo-Kitihara equation is sometimes easier to handle than the original master equation.

Note that, from this canonical homogeneous description, off stoichiometry ($c\neq 0.5$), one can compute (see Fig. 9) the stability boundary between the ordered and disordered phases *constrained to remain at the same fixed composition:* This is analogous to the T_0 line for thermodynamic systems. For allowing the existence of two-phase states as observed in Sec. II, two approaches are possible: either using a heterogeneous canonical description or a homogeneous grand-canonical description. Although the former approach is a simple extension of the one recalled in Sec. III A, the dimensionality of the order parameter is proportional to the cell number n_c so that the Kubo-Matsuo-Kitihara equation becomes difficult to solve. Note that numerical integration of the master equation allows one to assess the relative stability of competing states, without any assumption on the existence of a stochastic potential.[31] In the next section, we will introduce in detail an approach for building a homogeneous grand-canonical description that has been presented in a shortened version elsewhere.[32]

B. Grand-canonical homogeneous description

We consider here a grand-canonical ensemble where the total number of atoms in the system is fixed, but where the atomic concentration can vary. The main question concerns the way of building the dynamics of concentration changes: Since the microscopic detailed balance property is in general not fulfilled in driven systems, the choice for this dynamics—the number of atoms concerned in an exchange with the particle reservoir and attempt frequency for such jumps—will affect the kinetics and therefore the steady states reached by the system. We introduce now an approach where the dynamics of the canonical system [Eqs. (1) and (2) or (21) and (22)] provides enough physical information for building a grand-canonical description. This is performed by adapting the standard procedure for building grand-canonical equilibrium ensembles to the case of dynamical systems. By construction, the homogeneous canonical description and the grand-canonical one will be fully consistent; e.g., when the system at a given composition is found to remain single phase, its steady-state long-range-order parameter is the same in both descriptions. We will see that (i) outside irradiation, one recovers classical thermodynamic results, and (ii) under irradiation, we obtain a relationship between the canonical and grand-canonical stochastic potentials which generalized the Legendre transformation for thermal systems. The major limitation of this derivation is the assumption that no spatial organization takes place in the system.

1. *Dynamics of composition changes in a thermal system*

We will now use the notations used in Sec. II A: The bcc lattice is decomposed into two simple cubic sublattices (of Ω sites each), containing, respectively, N^{α} and N^{β} A atoms. The atomic occupancies on these sublattices are $C^{\alpha}=N^{\alpha}/\Omega$ and $C^{\beta}=N^{\beta}/\Omega$. As before, we restrict ourselves to nearest-neighbor interactions, and here, to simplify the calculations, we will assume that $V_{aa}=V_{bb}$ (as was done in all numerical computations reported in Sec. II).

Let us first introduce a procedure for building a grand-canonical ensemble for a thermal system starting from kinetic considerations: We consider two canonical systems $\mathcal{S}$ and $\mathcal{S}_0$ in contact at a temperature T, and we compute the rates of permutations according to the canonical dynamics of Sec. III A. When the A-B pair to be permuted belongs to the system $\mathcal{S}$, one gets the transition rates $W_{\pm s}$ for the dynamics of the degree of long-range-order S analogous to those of Eq. (22):

$$W_{+s}(\mathcal{N})=z\nu\Omega C^{\beta}(1-C^{\alpha})\Gamma\exp\left[\frac{\omega S}{kT}\right]\ , \quad (26a)$$

$$W_{-S}(\mathcal{N})=z\nu\Omega C^{\alpha}(1-C^{\beta})\Gamma\exp\left[-\frac{\omega S}{kT}\right]\ , \quad (26b)$$

with

$$\Gamma=\exp\left[-\frac{E_s}{kT}+\frac{z(V_{aa}+V_{bb}+2V_{ab})}{2kT}\right]=\frac{\Gamma_t}{\nu}\ . \quad (27)$$

When the atoms of the A-B pair are shared by $\mathcal{S}$ and $\mathcal{S}_0$, the exchange will result in a net change of composition in $\mathcal{S}$; the transition rates for the concentration dynamics are

$$W^{\alpha}_{+c}(\mathcal{N},\mathcal{N}_0)=z\nu_0\Omega(1-C^{\alpha})\Gamma\exp\left[\omega\frac{\frac{1}{2}-C^{\beta}}{kT}\right]\times C_0^{\beta}\exp\left[-\omega\frac{\frac{1}{2}-C_0^{\alpha}}{kT}\right]\ , \quad (28a)$$

$$W^{\alpha}_{-c}(\mathcal{N},\mathcal{N}_0)=z\nu_0\Omega C^{\alpha}\Gamma\exp\left[-\omega\frac{\frac{1}{2}-C^{\beta}}{kT}\right]\times(1-C_0^{\beta})\exp\left[\omega\frac{\frac{1}{2}-C_0^{\alpha}}{kT}\right]\ , \quad (28b)$$

when the atom belonging to the system $\mathcal{S}$ before the exchange is a B atom [Eq. (28a)] and an A atom [Eq. (28b)] on the sublattice α; similar expressions are obtained for $W^{\beta}_{\pm c}$ by exchanging α and β in Eqs. (28); the subscript 0 in Eqs. (28) refers to variables of the system $\mathcal{S}_0$. The activation energy for this jump has been computed as in Sec. II A [see Eqs. (3) and (4)] assuming that the atom of each system is surrounded by atoms belonging to the same system, which in a spatial picture would correspond to an abrupt interface between the two systems. Note that the attempt frequency ν_0 for chemical changes [Eq.

(28)] is not simply related to any physical quantity, contrary to the case of the attempt frequency ν, for long-range-order evolution [Eq. (26)], which is the Debye frequency in the system $\mathcal{S}$.

Now we let $\mathcal{S}_0$ become very large with respect to $\mathcal{S}$, so that $\mathcal{S}_0$ acts as a particle reservoir. The variables relative to the reservoir in Eqs. (28) are therefore no longer modified by the A-B exchange, and they characterize the reservoir. We assume now that the reservoir is at equilibrium: Minimizing the Bragg-Williams free energy $\mathcal{F}$ [Eq. (9)] with respect to the long-range-order parameter S_0 yields

$$2\frac{\omega}{kT}(C_0^\alpha - C_0^\beta) = \ln\left[\frac{C_0^\alpha(1-C_0^\beta)}{(1-C_0^\alpha)C_0^\beta}\right] . \tag{29a}$$

Let us define δ as

$$\delta = \ln\left[\frac{C_0^\beta}{1-C_0^\beta}\right] + \omega\frac{2C_0^\alpha - 1}{kT}$$
$$= \ln\left[\frac{C_0^\alpha}{1-C_0^\alpha}\right] + \omega\frac{2C_0^\beta - 1}{kT} , \tag{29b}$$

where the equilibrium relation [Eq. (29a)] has been used to get the last equality in Eq. (29b). Equations (28) can then be written as

$$W^\alpha_{+c}(\mathcal{N}) = z\nu_0\Omega[C_0^\beta(1-C_0^\beta)]^{1/2}(1-C^\alpha)\Gamma \times \exp\left[\omega\frac{\frac{1}{2}-C^\beta}{kT}\right]\exp\left[+\frac{\delta}{2}\right] , \tag{30a}$$

$$W^\alpha_{-c}(\mathcal{N}) = z\nu_0\Omega[C_0^\beta(1-C_0^\beta)]^{1/2}C^\alpha\Gamma \times \exp\left[-\omega\frac{\frac{1}{2}-C^\beta}{kT}\right]\exp\left[-\frac{\delta}{2}\right] , \tag{30b}$$

$$W^\beta_{+c}(\mathcal{N}) = z\nu_0\Omega[C_0^\alpha(1-C_0^\alpha)]^{1/2}(1-C^\beta)\Gamma \times \exp\left[\omega\frac{\frac{1}{2}-C^\alpha}{kT}\right]\exp\left[+\frac{\delta}{2}\right] , \tag{30c}$$

$$W^\beta_{c}(\mathcal{N}) = z\nu_0\Omega[C_0^\alpha(1-C_0^\alpha)]^{1/2}C^\beta\Gamma \times \exp\left[-\omega\frac{\frac{1}{2}-C^\alpha}{kT}\right]\exp\left[-\frac{\delta}{2}\right] . \tag{30d}$$

As seen from Eq. (29b), the parameter δ is simply related to the difference in the chemical potentials of species A and B in a Bragg-Williams approximation through $\delta=(\mu_A-\mu_B)/kT$. The above way of building a particle reservoir leads therefore, in the case of a thermal system, to a concentration dynamics fulfilling thermodynamic detailed balance.[29]

2. *Nonequilibrium grand-canonical ensemble*

In the same spirit as what was done in Sec. II A 1, irradiation effects are modeled by considering that two dynamics are acting in parallel: a thermally activated one and a forced one. Now ballistic jumps contribute both to chemical disordering and to composition changes. In the present description, this is achieved by considering that the system is interacting with two reservoirs,[29] undergoing pair exchanges with probability p with a reservoir characterized by (δ,β) (where β is the inverse temperature) and with probability $(1-p)$ with a reservoir characterized by $(\delta'=\delta,\ \beta'=0)$. Indeed, as the energies involved are much larger in the ballistic exchanges than in the thermally activated ones, the situation is simplified by treating the ballistic jumps as atomic jumps at infinite temperature [$\beta'=0$, as already done in Eqs. (1) and (2)]. Furthermore, in a high-temperature limit (β tending to zero), ballistic jumps are no longer physically distinguishable from thermal jumps in the alloy, and one thus should recover an infinite-temperature equilibrium description whatever the probability p: This implies $\delta'=\delta$.

The total rate of pair exchanges for the driven system is given by $\mathcal{W}=pW+(1-p)W'$, and consistently with Eq. (11), the intensity of external forcing is measured by the ratio of the ballistic jump frequency to an average thermal jump frequency: $\gamma=(1-p)/(p\Gamma)$.

As we have built the dynamics for the driven system, based on Eqs. (26)–(28), we can now write the master equation [Eq. (20)] or the Kubo-Matsuo-Kitihara equation [Eq. (25)] for the grand-canonical description:

$$\frac{\partial\Phi(n,t)}{\partial t} = w_{+s}(n)\left\{\exp-\left[-4\frac{\partial\Phi}{\partial S}\right]-1\right\} + w_{-s}(n)\left\{\exp\left[4\frac{\partial\Phi}{\partial S}\right]-1\right\} + w^\alpha_{+c}(n)\left\{\exp\left[-2\frac{\partial\Phi}{\partial S}-\frac{\partial\Phi}{\partial C}\right]-1\right\}$$
$$+ w^\alpha_{-c}(n)\left\{\exp\left[2\frac{\partial\Phi}{\partial S}+\frac{\partial\Phi}{\partial C}\right]-1\right\} + w^\beta_{+c}(n)\left\{\exp\left[2\frac{\partial\Phi}{\partial S}-\frac{\partial\Phi}{\partial S}\right]-1\right\} + w^\beta_{-c}(n)\left\{\exp\left[2\frac{\partial\Phi}{\partial S}+\frac{\partial\Phi}{\partial C}\right]-1\right\}, \tag{31}$$

where the various transition probabilities are defined by $w(n)=\mathcal{W}(\mathcal{N})/2\Omega$ and $\Phi(n)$ will denote the solution to Eq. (31) under steady-state conditions.

For driven systems no analytical solution either for the master equation or Kubo-Matsuo-Kitihara equation [Eq. (31)] is known when the order parameter is not a scalar, as is the case here. It is established that, for Markovian processes, if a steady state exists for the probability distribution, then it is unique. It is clear from Eq. (31) that this solution Φ will depend on the ratio ν_0/ν. For the case of alloys under irradiation we considered here, consistency with a heterogeneous canonical description requires that one compute the potential Φ *in the limit* $\nu_0/\nu\to 0$. Indeed, in such a heterogeneous canonical sys-

tem, where spatial organization does not take place (see Sec. II B 2) and when the interface width remains finite (as observed in Figs. 6–8), the fraction of atoms lying on interfacial sites tends to zero (as $\Omega^{-1/3}$) in the large system-size limit ($\Omega \to \infty$), while the attempt frequency for pair permutation is the same for all pairs. Thus the frequency of attempts which could modify the overall composition of a phase is infinitely small compared with that of attempts within a given phase. In the homogeneous grand-canonical description derived here, this implies that ν_0/ν tends to zero as $\Omega^{-1/3}$. In the limit $\nu_0/\nu \to 0$, Eq. (31) only retains terms in $\partial\Phi/\partial S$:[33] We recover precisely the Kubo-Matsuo-Kitihara equation of a canonical system [see Eq. (25)]. Full consistency between the two descriptions for steady-state values of the order parameter and the fluctuations around them is thus achieved. Note that in the simple example chosen here, the Kubo-Matsuo-Kitihara equation for a canonical system can easily be solved,[11] so that $\partial\Phi/\partial S$ is known for all $\mathcal{N}$. However, $\partial\Phi/\partial C$ remains yet unknown in the limit $\nu_0/\nu \to 0$.

Before taking the limit $\nu_0/\nu \to 0$, by the use of symmetry properties of the order-parameter space, $\partial\Phi/\partial C$ can be computed when $S=0$. Indeed, disordered states ($S=0$) lie on a symmetry axis of $\mathcal{N}$ space (see Fig. 10): This axis is invariant under permutation of the labeling of the two sublattices; since the partial derivatives of Φ are assumed to be continuous,[27,28] $\partial\Phi/\partial S$ is *vanishing along this axis*,[34] whatever the value of ν_0/ν. Simple algebra then yields

$$\frac{\partial\Phi}{\partial C}(C,S=0)=\ln\left[\frac{\omega^{\alpha}_{+c}(n)}{\omega^{\alpha}_{-c}(n)}\right]=\ln\left[\frac{\omega^{\beta}_{+c}(n)}{\omega^{\beta}_{-c}(n)}\right], \qquad (32)$$

where the last equality holds because the transition probabilities ω are taken for $S=0$.

Collecting this information yields the following analytical expression for Φ, in the limit $\nu_0/\nu \to 0$:

$$\Phi(C,S)-\Phi(\tfrac{1}{2},0)=+\tfrac{1}{4}\int_0^S ds\,\ln\left[\frac{\omega_{+s}(n)}{\omega_{-s}(n)}\right] + \int_{1/2}^{C} dc\,\frac{\partial\Phi}{\partial C}(C,S=0)\,, \qquad (33)$$

where the first integral in the RHS of Eq. (33) is the canonical potential.[13]

Equation (33) generalizes for a driven system the Legendre transformation which links grand-canonical and canonical potentials in an equilibrium system (see the Appendix). In the framework of the present homogeneous mesoscopic description, such a relation holds whenever the disordered states lie on a symmetry axis of the order-parameter space; this relation is therefore not restricted to the mean-field approximation used here to get a tractable expression for the transition rates W or to a direct-exchange mechanism for atomic jumps. It is easily checked from Eq. (33) that, without irradiation ($\gamma=0$), Φ is identical to the thermodynamic grand potential in the mean-field approximation considered here, the Bragg-Williams one (see the Appendix).

Figure 11 illustrates the results of the above method to assess the relative stability of competing phases in the bcc alloy under discussion. Beyond a critical forcing, the transition becomes first order (see Fig. 2). In the region where the transition is first order, the knowledge of Φ allows us to build the coexistence field: At a given γ and T, we search for a δ value such that the two local maxima of Φ, corresponding to the two possible steady states (C,S) and (C',S'), have the same Φ value. Our assumption that no patterning occurs implies that these two phases, when in contact, will interact weakly. Then a system of average composition C_0 such that $C<C_0<C'$ will decompose (see Fig. 10) and the composition and the degree of order are obtained from Φ, and their proportions given by the lever rule. A slight discrepancy exists (1% difference for the temperature of the congruent point at $\gamma=4.55$) between this phase diagram and the one computed from the heterogeneous deterministic model [Fig.

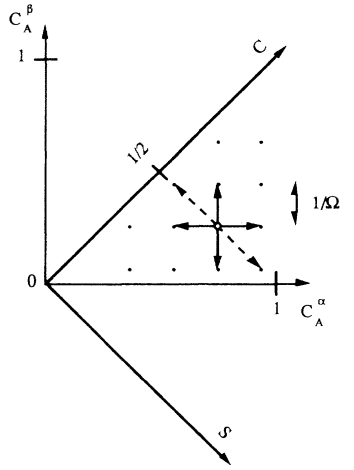

FIG. 10. Schematic drawing of the order-parameter space in the grand-canonical description. The various dynamics are represented by arrows linking sites of the discrete order-parameter space: long-range-order changes (dashed arrows) and concentration changes (solid arrows). The grid size ($1/\Omega$) has been exaggerated for sake of clarity.

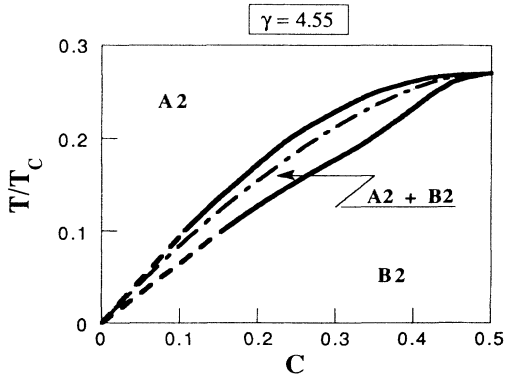

FIG. 11. Two-phase field at fixed forcing (solid line) and the "T_0 line" (long-short-dashed line) beyond the tricritical line, as computed from the stochastic potential Φ. Dashed lines correspond to extrapolation of the calculations.

3(a)]. This difference arises from the fact that some short range exists in the heterogeneous (deterministic) model, while it is absent from the homogeneous (stochastic) model;[35] such differences already exist for thermal systems.

Note that producing the ballistic jumps by cascade, instead of the uncorrelated jumps considered here, affects the first-order transition lines[13] and thus should affect the coexistence field. The existence of cascades of replacement modifies the dynamics of the system:[13,26] For the concentration evolution, the system may now exchange more than one atom at once with the infinite-temperature particle reservoir; the derivation of this new dynamics is, however, a simple extension of the method described above. This is left for future work.

IV. DISCUSSION AND CONCLUSION

Alloys under irradiation are examples of systems maintained in far-from-equilibrium situations by dynamical external forcing. As a result, such systems may exhibit states or behaviors which have no counterpart under purely thermal conditions. For the simple $A2$-$B2$ order-disorder transition on a bcc lattice, from a heterogeneous deterministic kinetic description we have shown that beyond a critical forcing intensity (i.e., beyond a critical irradiation flux) an alloy which is always single phase at equilibrium becomes two phase under steady-state conditions; this new irradiation-induced phase transition results from the change from second to first order in the order-disorder transition and is therefore different from irradiation-induced heterogeneous or homogeneous precipitations.[36,37] Introducing a grand-canonical nonequilibrium ensemble from a stochastic kinetic description, we have shown that a grand potential can be derived for the stationary probability distribution of ordered states; from this description we get a dynamical equilibrium phase diagram in good agreement with the deterministic one [compare Figs. 3(a) and 10] and confirming the existence of the two-phase field.

It is remarkable that this system—always homogeneous at equilibrium—can become *two phase* under an external forcing which usually is assumed to homogenize atomic configurations. Transitions which are second order at equilibrium can, under certain conditions, become first order under an external forcing. Gonzalez-Miranda *et al.*[2] and Dickman[3] have found such a behavior for a ferromagnetic Ising model with two dynamics acting in parallel: an infinite-temperature Kawasaki dynamics and a finite-temperature Metropolis dynamics. In the latter model, the behavior can be rationalized by the fact that the efficiency of the spin-exchanging Kawasaki dynamics inside a ferromagnetic domain is almost negligible compared with that at a domain boundary.[3] However, such a rationalization does not hold for an antiferromagnetic system, which is analogous to our model alloy.

For a two-phase alloy, we have identified a mechanism for APB elimination which leads to precipitate dissolution and redistribution under irradiation. Under irradiation, dislocation loops formed by point-defect agglomeration are growing and thus could shear ordered precipitates: Indeed, Potter and McCormick[38] observed such a shearing of γ' precipitates in NiAl (12% at. % Ni) under Ni^+ irradiation. Furthermore, they observed that this shearing induces a precipitate dissolution which was interpreted in terms of coupling between solute and vacancy fluxes toward the loop.[39] The mechanism observed in our model, where point defects are not taken into account, offers an alternative explanation.

Among the behaviors we have observed, some are nevertheless reminiscent of thermal behaviors. This is the case for the surface-tension and coarsening effects observed in Sec. II B 2. The knowledge of a stochastic potential for the heterogeneous case would allow one to derive and compute a surface tension, similarly to what was done for equilibrium systems.[40] Note also that the system under consideration here does not exhibit spatial organization.

Numerical modelization is a powerful tool for studying the kinetic path in alloys (see the recent work by Chen and co-workers,[41–43] Fultz,[44,45] and Anthony and Fultz[46]). Let us stress that the choice of the kinetic model is crucial when studying driven systems: While for equilibrium studies any dynamics fulfilling the detailed balance property will drive the system to its proper equilibrium state, the details of the kinetics will affect the steady states reached under forcing. We choose here kinetics according to rate theory [see Eqs. (1) and (2) and Fig. 1], which should be more realistic for thermally activated processes than kinetics where the activation energy atomic jumps mix energies of the initial and final configurations. Note that the results obtained are specific to the choices we made for the kinetic description: (i) a constant saddle-point configuration energy E_s, (ii) $V_{aa}=V_{bb}$ (used for numerical applications), and (iii) a direct exchange mechanism for modeling atomic diffusion. For homogeneous fcc driven systems, assumption (i) made here for simplicity is known to modify significantly the dynamical equilibrium phase diagram,[12] leading to the stabilization of new phases, while assumption (ii) is expected to have less severe an effect (for a thermal system, Fultz[45] has shown that this assumption modifies slightly the kinetics of $B2$ ordering in homogeneous systems). The choice of the mechanism for the atomic diffusion [assumption (iii)] is expected to influence strongly the kinetics of our systems (see Refs. 45 and 47 for comparative studies in thermal systems). Nevertheless, some features observed in this model seem to be generic. Indeed, Monte Carlo simulations, performed for an equiatomic bcc alloy under irradiation, have, however, shown that the $A2$-$B2$ transition changes from second order (at equilibrium) to first order (beyond a threshold in external forcing) whether atomic diffusion proceeds by a direct-exchange mechanism or by a vacancy-assisted mechanism.[14] Furthermore, for the case of alloys under irradiation considered here, diffusion through interstitial or interstitialcy mechanisms is to be taken into account, so that both vacancies and interstitials should be introduced in the description; this is left for future work.

In conclusion, from deterministic or stochastic kinetic descriptions, we show that irradiation stabilizes two-phase steady states in a bcc binary alloy presenting an $A2$-$B2$ order-disorder transition, the equilibrium phase

diagram of which only displays single-phase fields. Interface properties in this irradiation-stabilized two-phase field are studied: Surface-tension-like effects and coarsening are observed. APB's are unstable, and they get dissolved by the surrounding solid disordered solution; the smaller half of the ordered precipitate redissolves to the benefit of the larger one. From the stochastic kinetic description, the relative stability of competing locally stable steady states is computed by introduction of a grand-canonical ensemble for driven systems: The two-phase state, when it exists, is indeed found to be the more stable one. Irradiation experiments will be useful for assessing the relevance of our description for real systems.

ACKNOWLEDGMENTS

Useful discussions with Dr. F. Haider, Dr. A. Khoutami, Dr. B. Legrand, Dr. E. Salomons, Dr. A. Senhaji, and Dr. G. Tréglia are gratefully acknowledged.

APPENDIX: RELATIONSHIP BETWEEN GRAND-CANONICAL AND CANONICAL POTENTIALS FOR DRIVEN AND THERMAL SYSTEMS

We give here the detailed expression of the grand-canonical potential for a driven system, and we checked that without irradiation, i.e., $\gamma=0$, one recovers the usual thermodynamic grand potential, in the Bragg-Williams approximation.

Inserting Eqs. (26) and (30) into Eq. (33) yields, for $\Delta\Phi(C,S)=\Phi(C,S)-\Phi(\frac{1}{2},0)$,

$$\Delta\Phi(C,S)=-\tfrac{1}{2}\{C^{\alpha}\ln C^{\alpha}+C^{\beta}\ln C^{\beta}+(1-C^{\alpha})\ln(1-C^{\alpha})+(1-C^{\beta})\ln(1-C^{\beta}+2\ln 2\}$$
$$+\tfrac{1}{4}\int_0^S ds\,\ln\left[\frac{e^{\omega s/kt}+\gamma}{e^{-\omega s/kT}+\gamma}\right]+\int_{1/2}^{C} dc\,\ln\left[\frac{e^{\omega(1/2-c)/kT}+\gamma}{e^{-\omega(1/2-c)/kT}+\gamma}\right]+\delta(C-\tfrac{1}{2})\,, \tag{A1}$$

where s and c are the current values of S and C, and with $C^{\alpha}=C+S/2$ and $C^{\beta}=C-S/2$.

Without irradiation, we set $\gamma=0$ in Eq. (A1); this yields

$$\Delta\Phi_{\gamma=0}(C,S)=-\tfrac{1}{2}\{C^{\alpha}\ln C^{\alpha}+C^{\beta}\ln C^{\beta}+(1-C^{\alpha})\ln(1-C^{\alpha})+(1-C^{\beta})\ln(1-C^{\beta})+2\ln 2\}$$
$$+\frac{\omega S^2}{4kT}-\frac{\omega(C-\frac{1}{2})^2}{kT}+\delta(C-\tfrac{1}{2}) \tag{A2}$$
$$=-\frac{1}{kT}[\Delta\mathcal{F}(C,S)-(\mu_A-\mu_B)(C-\tfrac{1}{2})]\,, \tag{A3}$$

where the free energy $\mathcal{F}(C,S)$ is the one introduced in Eq. (9) and with the use of the relation between δ and the equilibrium chemical potential [see Eq. (30)]. Equation (A3) shows that the kinetic description derived for a grand-canonical nonequilibrium ensemble, when specified to a thermal case, is consistent with equilibrium thermodynamic description.

Under irradiation, at steady state, $\Delta\Phi$ is extremum, so that $\partial\Delta\Phi/\partial C^{\alpha}=\partial\Delta\Phi/\partial C^{\beta}=0$. This yields the following expression for the effective chemical potential:

$$\delta=\ln\left[\frac{C^{\alpha}}{1-C^{\alpha}}\right]-\frac{1}{2}\ln\left[\frac{e^{\omega s/kT}+\gamma}{e^{-\omega s/kT}+\gamma}\right]-\ln\left[\frac{e^{\omega(1/2-c)/kT}+\gamma}{e^{-\omega(1/2-c)/kT}+\gamma}\right]$$
$$=\ln\left[\frac{1-C^{\beta}}{c\beta}\right]+\frac{1}{2}\ln\left[\frac{e^{\omega s/kT}+\gamma}{e^{-\omega s/kT}+\gamma}\right]-\ln\left[\frac{e^{\omega(1/2-c)/kT}+\gamma}{e^{-\omega(1/2-c)/kT}+\gamma}\right]. \tag{A4}$$

The last equality is fulfilled at steady state: It is indeed obtained by setting $dC^{\alpha}/dt=0$ in Eq. (7). The effective chemical potential for the system under irradiation is therefore found to be the same on both sublattices.

[1]K. C. Russell, *Phase Stability Under Irradiation,* Progress in Materials Science (Pergamon, Oxford, 1984), Vol. 18, p. 229.
[2]J. M. Gonzalez-Miranda, P. L. Garrido, J. Marro, and J. L. Lebowitz, Phys. Rev. Lett. **59**, 1934 (1987).
[3]R. Dickman, Phys. Lett. A **122**, 463 (1987).
[4]F. Schlögl, Phys. Rep. **62**, 267 (1980).
[5]R. Landauer, J. Appl. Phys. **33**, 2209 (1962).
[6]S. Katz, J. L. Lebowitz, and H. Spohn, Phys. Rev. B **28**, 1655 (1983).
[7]G. Martin, Phys. Rev. B **30**, 1424 (1984).
[8]E. M. Schulson, J. Nucl. Mater. **83**, 239 (1979).
[9]S. Banerjee and K. Urban, Phys. Status Solidi **81**, 145 (1985).
[10]K. Y. Liou and P. Wilkes, J. Nucl. Mater. **87**, 317 (1979).
[11]P. Bellon and G. Martin, Phys. Rev. B **38**, 2570 (1988).
[12]F. Haider, P. Bellon, and G. Martin, Phys. Rev. B **42**, 8274 (1990).
[13]P. Bellon and G. Martin, Phys. Rev. B **39**, 2403 (1989).
[14]E. Salomons, P. Bellon, F. Soisson, and G. Martin, Phys. Rev. B **45**, 4582 (1992).
[15]H. Ackermann, G. Inden, and R. Kikuchi, Acta Metall. **37**, 1

(1989).
[16]G. J. Dienes, Acta Metall. **3**, 549 (1955).
[17]G. H. Vineyard, Phys. Rev. B **102**, 981 (1956).
[18]J.-C. Tolédano and P. Tolédano, *The Landau Theory of Phase Transitions* (World Scientific, Singapore, 1987).
[19]W. H. Press, B. P. Flannery, S. A. Teukolsky, and W. T. Vetterling, *Numerical Recipes: The Art of Scientific Computing* (Cambridge University Press, Cambridge, England, 1986).
[20]Long-Qing Chen and A. G. Khachaturyan, Scr. Metall. **25**, 61 (1991).
[21]R. Sizman, J. Nucl. Mater. **69&70**, 386 (1978).
[22]G. Inden, Acta Metall. **22**, 945 (1974).
[23]G. Martin, Phys. Rev. B **41**, 2279 (1990).
[24]G. Nicolis and I. Prigogine, *Self-Organization in Nonequilibrium Systems* (Wiley, New York, 1977).
[25]H. Haken, *Advanced Synergetics* (Springer, Berlin, 1983).
[26]P. Bellon, F. Haider, and G. Martin, in *Proceedings of the International Conference on Radiation Material Science* (Alushta, 1990), edited by V. F. Zelensky (Physical and Technical Institute, Kharkov, 1990); J. Nucl. Mater. (to be published).
[27]R. Görtz, Physica **90A**, 360 (1978).
[28]R. Kubo, K. Matsuo, and K. Kitihara, J. Stat. Phys. **9**, 51 (1973).
[29]M. Suzuki, Prog. Theor. Phys. **53**, 1657 (1975); **55**, 383 (1976).
[30]J. L. Lebowitz and P. G. Bergmann, Ann. Phys. (N.Y.) **1**, 1 (1957).
[31]F. Haider, in *Ordering and Disordering in Alloys,* edited by A. R. Yavari (Elsevier, New York, 1991).
[32]P. Bellon, Phys. Rev. B **45**, 7517 (1992).
[33]To get this result, the partial derivatives of Φ have been assumed to be continuous when $\nu_0/\nu \rightarrow 0$.
[34]Other examples of the use of symmetry properties for simplifying or solving the Kubo-Matsuo-Kitihara equation can be found in Ref. 12.
[35]P. Bellon, F. Soisson, G. Martin, and F. Haider (unpublished).
[36]A. Barbu and A. J. Ardell, Scr. Metall. **9**, 1233 (1975).
[37]R. Cauvin and G. Martin, Phys. Rev. B **23**, 3322 (1981); **23**, 3333 (1981); **25**, 3385 (1982).
[38]D. I. Potter and A. W. McCormick, Acta Metall. **933** (1979).
[39]D. I. Potter and H. Wiedersich, J. Nucl. Mater. **83**, 208 (1979).
[40]J. W. Cahn and J. E. Hilliard, J. Chem. Phys. **28**, 258 (1958).
[41]L.-Q. Chen and A. G. Kachaturyan, Scr. Metall. **25**, 61 (1991); **25**, 67 (1991).
[42]Y. Wang, L.-Q. Chen, and A. G. Khachaturyan, Scr. Metall. **25**, 1387 (1991); **25**, 1969 (1991).
[43]L.-Q. Chen and A. G. Khachaturyan, Phys. Rev. B **44**, 4681 (1991).
[44]B. Fultz, Acta Metall. **37**, 823 (1989).
[45]B. Fultz, J. Mater. Res. **5**, 1419 (1990).
[46]L. Anthony and B. Fultz, J. Mater. Res. **4**, 1132 (1989); **4**, 1140 (1989).
[47]E. Vives and A. Planes, Phys. Rev. Lett. **68**, 812 (1992).

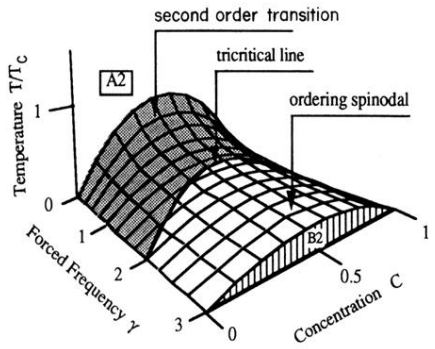

FIG. 2. Dynamical equilibrium phase diagram for a bcc alloy in ($T \times \gamma \times C$) space. For clarity, when the transition is first order, only the spinodal is displayed. γ is dimensionless Eq. (11).

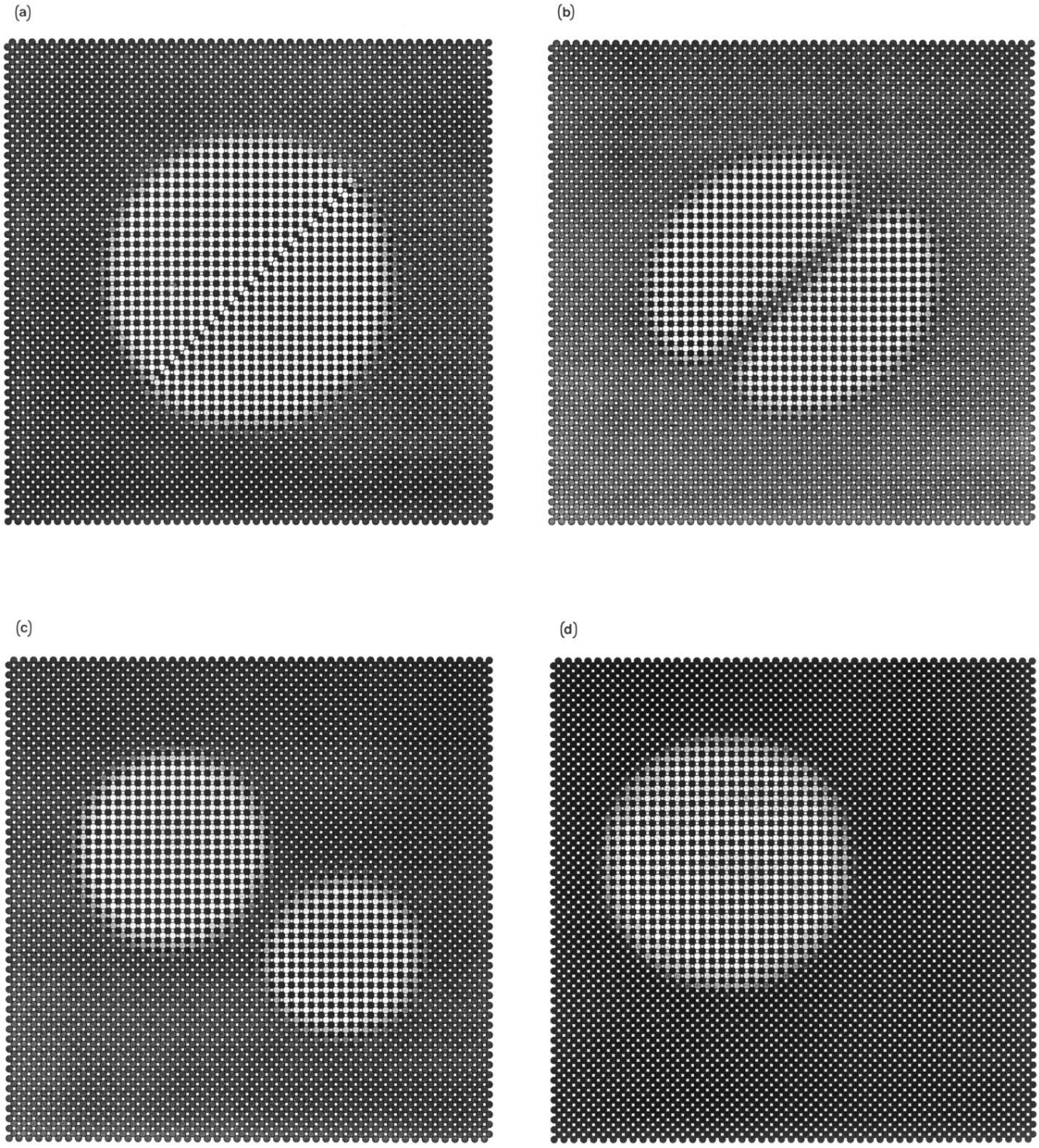

FIG. 6. Evolution of an ordered precipitate after a conservative APB introduction in a thermal system. $T/T_c = 0.25$ and $\gamma = 0$. The concentrations at lattice sites are visualized by the darkness of the circles. The maxima of A atomic concentrations (here close to 0.98) are represented by the darkest circles, and the minima (here close to 0.02) are represented by the lightest circles. In arbitrary time units (a) $t = 0$, (b) $t = 1$, (c) $t = 300$, and (d) $t = 900$.

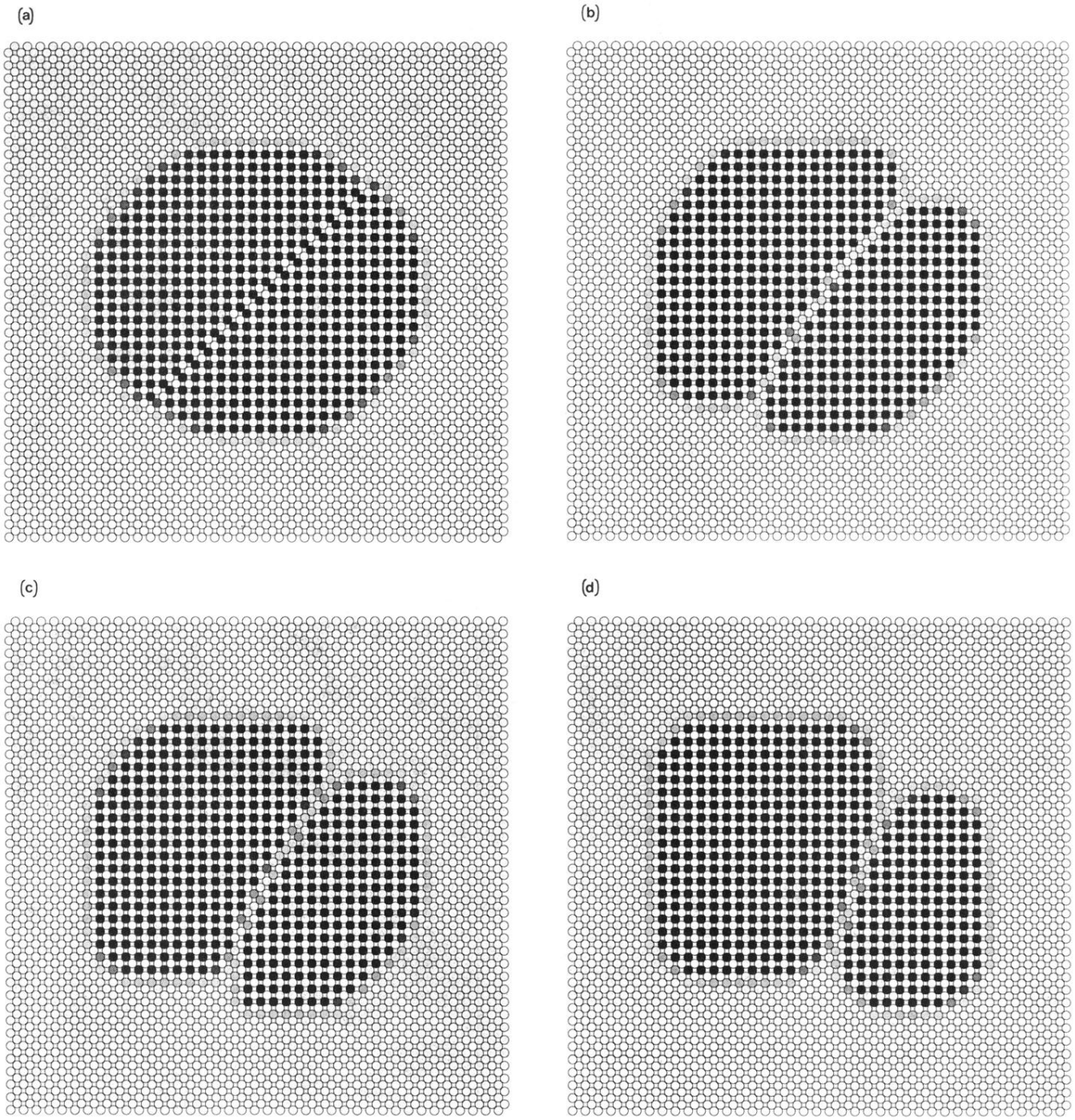

FIG. 7. Evolution of an ordered precipitate after conservative APB introduction in a driven system. $T/T_c = 0.20$ and $\gamma = 4.55$. The concentrations at lattice sites are visualized by the darkness of the circles. The maxima of A atomic concentration (here close to 0.67) are represented by the darkest circles, and the minima (here close to 0.01) are represented by the lightest circles. In arbitrary time units (a) $t = 0$, (b) $t = 1760$, (c) $t = 2660$, and (d) $t = 8960$.

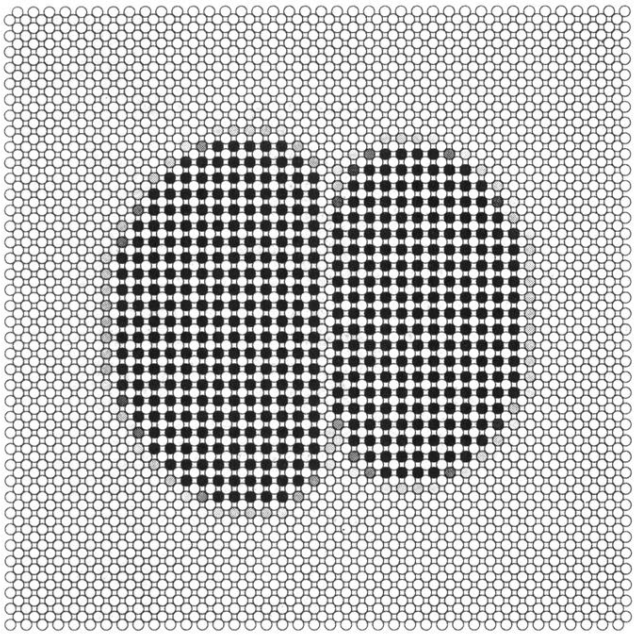

FIG. 8. Steady-state ordered precipitate after a nonconservative APB introduction in a thermal system. $T/T_c=0.25$ and $\gamma=0$.